*Peremennye Zvezdy* (*Variable Stars*) **45**, No. 3, 2025

Received 3 January; accepted 24 January.

DOI: 10.24412/2221-0474-2025-45-32-44

# Photometric Study of New and Suspected Binary Stars in the Fields of V0873 Per and CV Boo

A.V.Khalikova[1], E.R. Gaynullina[1], A.V. Serebryanskiy[2], B.L. Satovskiy[3]

[1] Ulugh Beg Astronomical Institute, Uzbek Academy of Sciences, Astronomicheskaya Str. 33, 100072, Tashkent, Uzbekistan; e-mails: ahalikova@astrin.uz, evelina@astrin.uz

[2] Fesenkov Astrophysical Institute, Observatory 23, 050020, Almaty, Kazakhstan; e-mail: alex@aphi.kz

[3] State Space Corporation "Roscosmos", Moscow, Russia

Six binary and candidate binary stars in the fields of V0873 Per and CV Boo were found using archive observations of the Mt. Maidanak Astronomical Observatory. (1) 2MASS J02465266+4125290 is a detached eclipsing binary with the period of $P = 5\overset{\mathrm{d}}{.}9436 \pm 0\overset{\mathrm{d}}{.}0027$. (2) TYC 2853-60-1 is a detached eclipsing binary with the period of $P = 1\overset{\mathrm{d}}{.}79 \pm 0\overset{\mathrm{d}}{.}01$. (3) 2MASS J02475840+4116103 is an ellipsoidal binary system with the period of $P = 0\overset{\mathrm{d}}{.}30744 \pm 0\overset{\mathrm{d}}{.}00005$. (4) 2MASS J02464361+4120282 is a BY Dra-type binary star with the rotational period of $P = 12\overset{\mathrm{d}}{.}18 \pm 0\overset{\mathrm{d}}{.}06$. (5) 2MASS J02465622+4117392 is an ellipsoidal binary system with the period of $P = 4\overset{\mathrm{d}}{.}022 \pm 0\overset{\mathrm{d}}{.}009$. (6) 2MASS J15273711+3703070 is an ellipsoidal and/or RS CVn binary system with the period of $P = 0\overset{\mathrm{d}}{.}3307 \pm 0\overset{\mathrm{d}}{.}0002$. Three of these stars exhibit chromospheric activity.

## 1 Introduction

Several known eclipsing binaries have been observed at Mt. Maidanak Astronomical Observatory (MAO) in Uzbekistan. In 2013 and 2014, the observations were carried out in the frame of the SPAREBIS (Search for Planets Around Eclipsing Binary Stars) project initiated by Tutukov & Bogomazov (2012). Some stars were additionally observed in 2015. The field of V0873 Per was observed in 2013, 2014, and 2015 (45 nights in total). Several stars have been suspected of being variable during data processing and analysis, which included machine learning methods. As a result, we have been able to confirm five variable stars. CV Boo was observed during 41 nights in May–July, 2014. After cross-identification of stars around CV Boo with catalogs of suspected variable stars, we confirmed variability for one of our discoveries. The paper presents the results of our study of those objects that we classified as binary or candidate binary stars. In Section 2, we describe the observations and data processing. In Section 3, we describe data analysis and our results. The conclusions are summarized in Section 4.

## 2 Observations and data reduction

The field of V0873 Per was observed during 22 nights in 2013, 7 nights in 2014, and 16 nights in 2015. All observations were carried out using the 60 cm Zeiss-600 North telescope with the focal length of 7200 mm, equipped with an FLI MicroLine CCD, with a Kodak KAF-1001E chip. The scale was $0\overset{''}{.}687$ per pixel, providing the field of view (FoV) of $11\overset{'}{.}7 \times 11\overset{'}{.}7$. The observations were performed in the Bessel $R$ filter. The typical exposure times were 25–40 seconds. The average Full Width at Half Maximum (FWHM) in each observing season was $2\overset{''}{.}04$, $1\overset{''}{.}87$, $2\overset{''}{.}13$ for 2013, 2014, and 2015, respectively. The number

Table 1: Basic information about the comparison and check stars

| Stars | ID | $\alpha$(J2000) [h:m:s] | $\delta$(J2000) [°:′:″] | $V$ [mag] | $B-V$ [mag] |
|---|---|---|---|---|---|
| | | V0873 Per field | | | |
| R1 | TYC 2853-294-1 | 02:47:18.02 | +41:23:07.4 | 10.97 (0.03) | 0.94 (0.04) |
| R2 | TYC 2853-312-1 | 02:47:08.41 | +41:20:49.7 | 11.27 (0.02) | 0.37 (0.03) |
| S1 | TYC 2853-744-1 | 02:47:21.96 | +41:23:08.2 | 12.08 (0.02) | 1.25 (0.04) |
| | | CV Boo field | | | |
| R3 | BD +37 2645 | 15:27:06.86 | +36:59:27.0 | 10.68 (0.10) | 0.57 (0.11) |
| S2 | TYC 2570-417-1 | 15:27:28.79 | +36:47:22.5 | 11.08 (0.09) | 1.07 (0.11) |

of stars measured each night was from 120 to 230 depending on the specific sky area in the telescope FoV. We calculated differential magnitudes using the same comparison stars as in Bogomazov et al. (2016a), TYC 2853 294-1 and TYC 2853-312-1 (R1 and R2, see Table 1) for different nights. The star TYC 2853-744-1 (S1) was used as a check star. These three stars are assumed to be non-variable during our observations.

The observations of the field of CV Boo were carried out during 34 nights in 2014 using the 51 cm AMT-1 telescope (AstroTel Ltd.) with the focal length of 4000 mm, equipped with Apogee Alta-U16M 4K×4K CCD, the light detector being a Kodak KAF-1001E chip. The scale was $0\farcs928$ per pixel, and the FoV was $31\farcm8 \times 31\farcm8$. Observations were performed in the Bessel $R$ filter. The typical exposure times were 8–20 seconds. The average FWHM was $2\farcs2$. We selected BD +37 2645 (R3) as the comparison star and TYC 2570-417-1 (S2) as the check star (Bogomazov et al. 2016b).

Basic image reductions (dark current and flat field corrections) were performed for both fields using standard IRAF[1] software. We applied differential photometry with the IRAF/DAOPHOT package. For uncertainties of instrumental magnitudes, we accepted the standard IRAF errors. No differential extinction corrections were applied.

Basic information for the comparison and check stars is provided in Table 1. The coordinates are given according to the GAIA DR3 catalog (Gaia Collaboration et al. 2021); $V$ magnitudes and $B-V$ color indices are from the AAVSO Photometric All Sky Survey (Henden et al. 2015).

# 3 Light curve analysis and results

## 3.1 The field of V0873 Per

The light curves were analyzed for variability using unsupervised clusterization methods. For photometric observations, especially for large-scale surveys, the same unsupervised machine learning model is an easy way to perform many different tasks (preliminary classification, selection of anomalies, dimension reduction, discovering hidden patterns in data), in variance to supervised machine learning model that is trained for a single specific task. We performed cluster analysis using our new light curve representation (Khalikova et al. 2022). We assumed that the clusters with one or two light curves (the so-called anomaly clusters) contain the light curves of stars that may be variable because their behavior differs from the bulk of the sample. After visual examination of the smallest clusters, we discovered that, indeed, some stars were possibly variable. In particular, one

[1]IRAF is distributed by the NOAO, which is operated by the AURA, Inc., under a cooperative agreement with the NSF.

of the stars turned out to be a detached binary star. Additionally, we cross-matched the stars in the field slightly larger than the telescope FoV with ATLAS (Heinze et al. 2018) and ZTF (Chen et al. 2020) catalogs of suspected variable stars and also extracted the publicly available light curves (sector 58) from TESS mission (Stassun et al. 2019). As a result, we selected several stars for further analysis as candidate binary stars.

#### 3.1.1 Star *a*: 2MASS J02465266+4125290

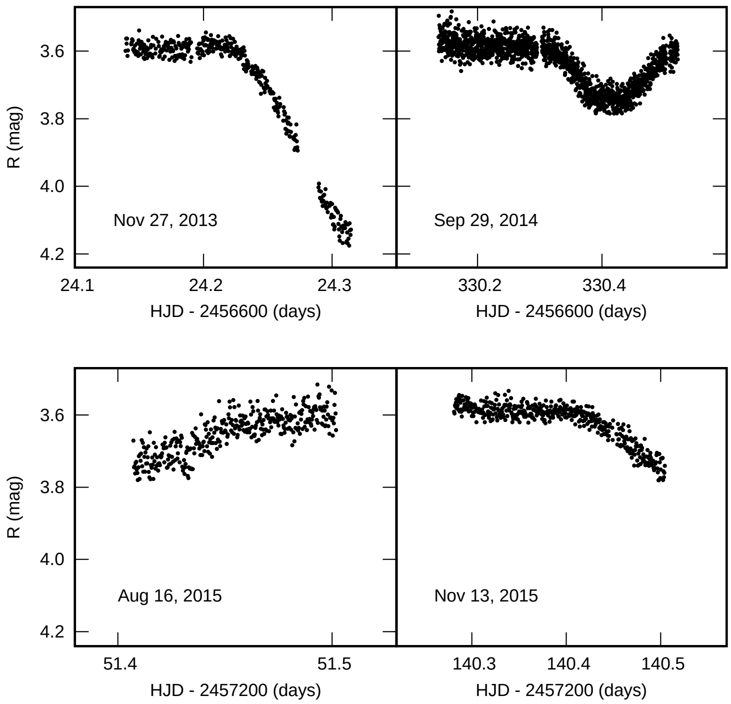


**Figure 1.**
The light curves of the star 2MASS J02465266+412590 (the star *a*) during 4 nights (MAO) showing variability.

The star *a* ($\alpha = 02^{\mathrm{h}}46^{\mathrm{m}}52\overset{\mathrm{s}}{.}66$, $\delta = +41°25'29\overset{''}{.}0$, J2000) is a member of the open star cluster NGC 1039 (Cantat-Gaudin et al. 2018). It was classified in the ATLAS catalog as “dubious”, with the periods from long-period Fourier and Lomb–Scargle fit being $P_{\mathrm{LF}} = 6\overset{\mathrm{d}}{.}0899$ and $P_{\mathrm{LS}} = 1\overset{\mathrm{d}}{.}1384$, respectively. According to Maíz Apellániz et al. (2023), this star has a variability flag VARF=“variable” but without classification. The light curves of this star from four MAO observing nights show that it is a detached eclipsing binary. These differential light curves are shown in Fig. 1. In the top left panel (November 27, 2013), we see a part of the primary eclipse; the other 3 nights demonstrate a secondary eclipse or a part of it.

In order to determine the orbital period, we applied the dispersion spectrum analysis (Pelt et al. 1994, 1996) to these 4 nights; namely, we used the dispersion spectra $D_2^2$, $D_3^2$, and $D_{4,k}^2$ with $k \sim 1,\ 2,\ 3,\ 4$. Then we calculated average values of the statistics for the time intervals between September 29, 2014 and August 15, 2015 and between September 29, 2014 and November 13, 2015. We obtain 320.967±0.001 days and 410.101±0.003 days, respectively. As the next step, we divided these time lags on integers because we assume

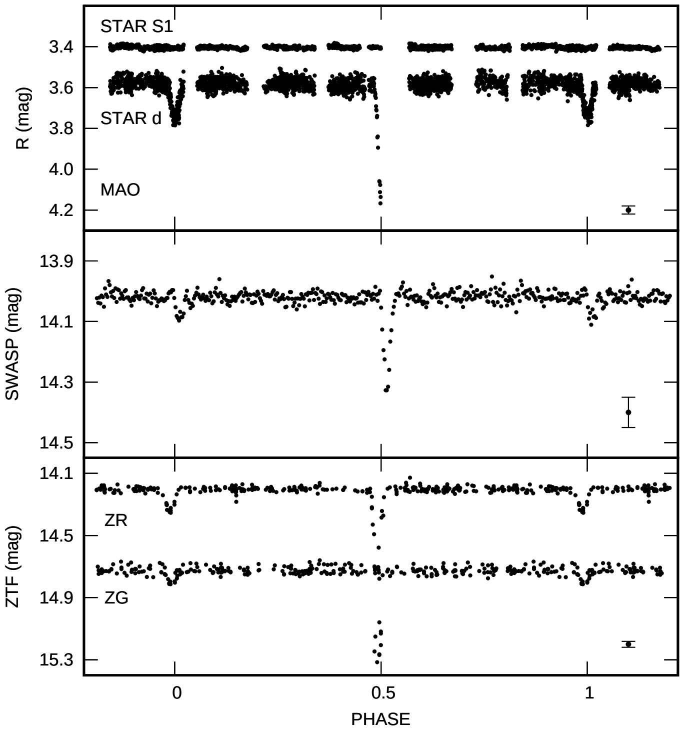


**Figure 2.**
Phase-folded MAO (top), SWASP (middle), and ZTF (bottom) light curves of the star 2MASS J02465266+412590 (the star *a*). The light curve of the star S1 was shifted by $+2^{\mathrm{m}}.4$. In the lower right corners, the typical uncertainties are given, but in the case of SWASP data, the mean standard deviation of points in bins is shown.

the integer number of the periods between the times of minima. Finally, we estimated the period of $P = 5^{\mathrm{d}}.944 \pm 0^{\mathrm{d}}.003$. This period is slightly shorter than that from the ATLAS, $P_{\mathrm{LF}}$: by $0^{\mathrm{d}}.146$. We used the observational data from September 29, 2014 to determine the time of minimum for the secondary eclipse because we have only a part of the primary eclipse. As in Gaynullina et al. (2019), our calculations of the time of minimum were performed in three different ways: with the conjunction method (Duerbeck 1975), with the 4th-order polynomial fit, and with the MINIMA27 code[2] that implements 6 different methods. The average of all values was calculated with the standard deviation as the uncertainty. Thus we obtained HJD(minII)$= 2456930.4136 \pm 0^{\mathrm{d}}.0026$.

The star *a* was observed in the SuperWASP Survey (SWASP, Butters et al. 2010) from July 2004 till December 2007 and in the ZTF Survey from July 2018 till November 2021. We have cleaned the SWASP light curves removing those data points where internal magnitude uncertainties exceeded $0^{\mathrm{m}}.1$. In Fig. 2, we show the MAO, SWASP, and ZTF phase light curves folded with the period of 5.944 days using the earlier determined HJD(minII) as the initial epoch. We used 33 more nights of MAO observations without signs of eclipses and also plotted the folded light curve of the check star S1. SWASP data are much noisier, therefore we present them averaged in bins, with 500 bins used. The SWASP and ZTF phase light curves show small offsets from phases 0 and 0.5. This means that we need more observations of eclipses to obtain a more precise ephemeris. From the MAO data, the other parameters for the secondary eclipse are: depth, $0^{\mathrm{m}}.162 \pm 0^{\mathrm{m}}.004$ (in *R*); duration, $0^{\mathrm{d}}.207 \pm 0^{\mathrm{d}}.007$. The depth of the primary eclipse is at least $0^{\mathrm{m}}.59$, and it lasts

[2] https://www.variablestarssouth.org/resources/bob-nelsons-software-tools/software-by-bob-nelson

about $0^{\rm d}.23$. More information about star *a* (and other studied stars) is given in Table 3.

#### 3.1.2 The star *b*: TYC 2853-60-1 or 2MASS 02461044+4123154?

The star TYC 2853-60-1, hereafter the star *b1* ($\alpha = 02^{\rm h}46^{\rm m}10^{\rm s}.08$, $\delta = +41^\circ 22' 33''.8$, J2000), is also a member of the open star cluster NGC 1039. According to Maíz Apellániz et al. (2023), its VARF is "marginal". The TESS publicly available light curve of the star *b1* shows very shallow and low-amplitude periodic changes. The frequency analysis was performed with FAMIAS (Zima 2008), the obtained period is $P = 1^{\rm d}.794 \pm 0^{\rm d}.008$. The folded light curve demonstrates a detached binary star with two eclipses, where the secondary eclipse shows up only slightly.

In Fig. 3, we show the phased light curve of the star folded with the period of 1.794 days as well as the smoothed curve. The initial epoch was $\mathrm{BJD}_0 = 2459883.8737$.

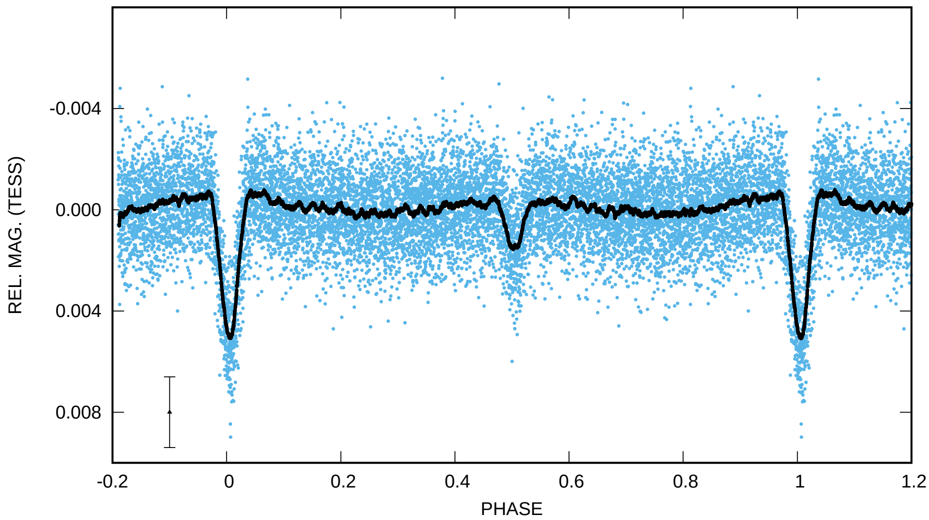


**Figure 3.**
The TESS light curve of TYC 2853-60-1 (star *b1*) folded with the period of $1^{\rm d}.794$ and the smoothed curve.

We performed binary star modeling with JKTEBOP (Southworth et al. 2004). The final best model implies a strong third light $L_3 = 0.98$ ($L_1 + L_2 + L_3 = 1$). Since the star *b1* is not included in the photometric catalogs of suspected variable stars, we came to the conclusion that another star could be variable because of a relatively large aperture radius of $1'.05$. Indeed, according to the ATLAS catalog, the star 2MASS 02461044+4123154, or star *b* ($\alpha = 02^{\rm h}46^{\rm m}10^{\rm s}.44$, $\delta = +41^\circ 23' 15''.4$, J2000), has $P_{\rm LF} = 27^{\rm d}.793756$ and $P_{\rm LS} = 3^{\rm d}.532946$ ("dubious" classification). A half of $P_{\rm LS}$ is $1^{\rm d}.76647$, which is close to our determined period. According to Maíz Apellániz et al. (2023), this star's VARF is "variable". Figure 4 shows the light curves from the ATLAS and ZTF surveys folded with the period $P = 1^{\rm d}.7947$ and epoch $\mathrm{BJD}_0 = 2459883.8747$, calculated with JKTEBOP from TESS data. Now the depth of the minimum during the primary eclipse is about $0^{\rm m}.4$, which is two orders of magnitude larger than that in the TESS data for the star *b1*. The considerable difference in the depths of the primary and secondary minima, $\sim 0^{\rm m}.28$ ($G$) and $\sim 0^{\rm m}.28$ ($R$), compared to $\sim 0^{\rm m}.016$ ($G$) and $\sim 0^{\rm m}.049$ ($R$), implies that the second star is much cooler.

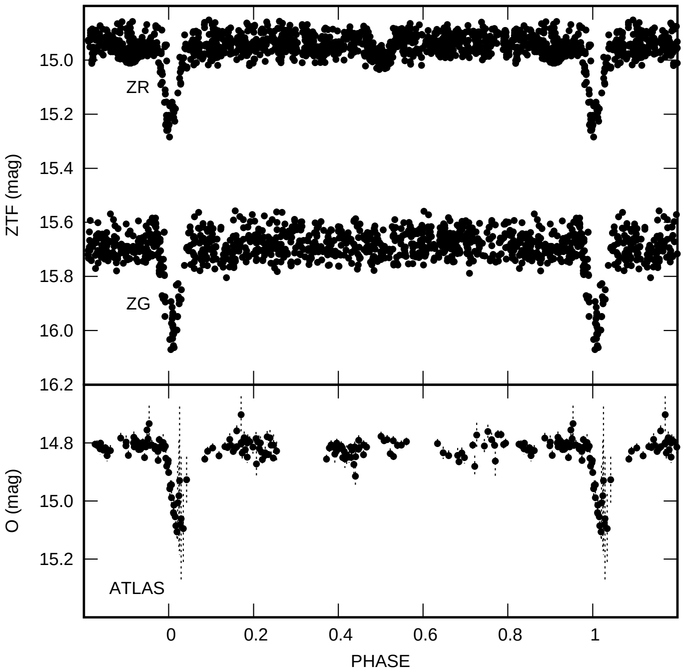


**Figure 4.**
The phased light curves of the star 2MASS 02461044+4123154 (the star *b*) calculated from ATLAS and ZTF data.

In Table 2, columns 2 and 3, we present the times of the primary minimum derived from the TESS light curve of the star *b1*. For this purpose, we used (a) Gauss function fitting (lmfit[3], Levenberg–Marquardt minimizer) and (b) MINIMA27 code. For the calculation of the new linear elements ($BJD_0$ and $P$), we used only those minima that included enough data points around minima without large gaps. As a result, 12 times of the primary minimum were used. The ephemeris determined by the least-squares solution is:

$$\mathrm{BJD(minI)} = 2459883.8746 \pm 0.0018 + (1\overset{\mathrm{d}}{.}7947 \pm 0\overset{\mathrm{d}}{.}0002)E.$$

The fourth column in Table 2 contains O–C values averaged for the two methods and calculated using these linear elements. $E$ is the epoch number. In Fig. 5, we plot the O–C values that show only weak signs of variation on the time scale about 20 days. Eclipse timing variations can have different nature, for example, the presence of an additional body in the system. To date, the shortest period for an exoplanet around the binary star (P-type system) is 43 days, and seven exoplanet candidates have possible periods shorter than 20 days. The third body model fit was performed with the OCFit software (Parimucha et al. 2018), the package for fitting O–C diagrams using Genetic Algorithms, and Markov chain Monte Carlo methods. The results are also shown in Fig. 5. We do not provide values for the model parameters because there is insufficient data to be confident. In order to verify periodic O–C changes, TESS light curves for the star $b$ are needed.

[3]https://lmfit.github.io/lmfit-py/

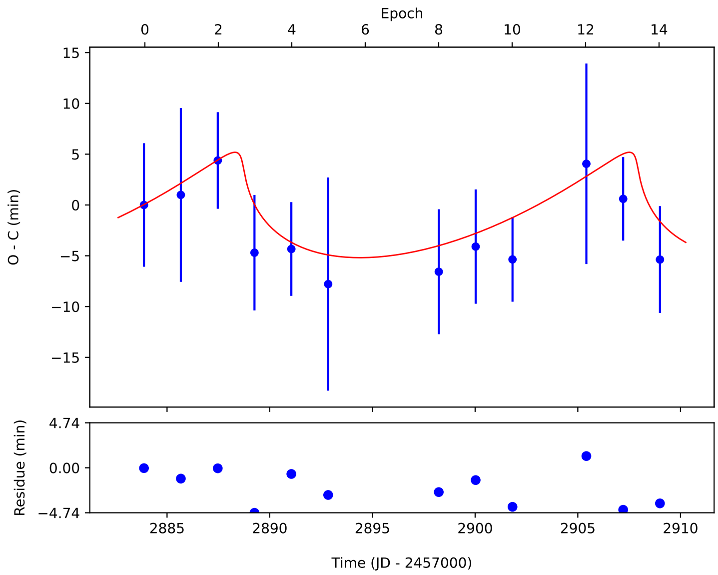


**Figure 5.**
O–C values (see Table 2) for the star $b$ and the possible third-body model fit with period $19\overset{\mathrm{d}}{.}22 \pm 0\overset{\mathrm{d}}{.}06$ and eccentricity 0.90±0.09.

### 3.1.3 The star $c$: 2MASS J02475840+4116103

The star $c$, or 2MASS J02475840+4116103 ($\alpha = 02^{\mathrm{h}}47^{\mathrm{m}}58\overset{\mathrm{s}}{.}40$, $\delta = +41^\circ16'10\overset{''}{.}3$, J2000), is located comparatively close to the Sun. According to Maíz Apellániz et al. (2023), the star has the flag VARF="variable". The star $c$ was included in the ZTF catalog of suspected variables, and its suspected periods are $P_g = 0\overset{\mathrm{d}}{.}30737$ and $P_r = 0\overset{\mathrm{d}}{.}30743$ for the $g$ and $r$ bands. The publicly available TESS light curve (sector 58) of the star $c$ shows small-amplitude variations of the flux. We analyzed the TESS light curve with FAMIAS. The Fourier spectrum presented in the top panel of Fig. 6 shows only two significant frequencies with a ratio $f_2/f_1$=2, which is typical of binary stars. The light curve folded with the period $P_1 = 0\overset{\mathrm{d}}{.}30744 \pm 0\overset{\mathrm{d}}{.}00005$ (that agrees well with the ZTF estimate) is also shown in Fig. 6. The phased light curve shows two minima, and the secondary one is much shallower.

### 3.1.4 The star $d$: 2MASS J02464361+4120282

According to GAIA DR3 (Pourbaix et al. 2022), the star $d$ ($\alpha = 02^{\mathrm{h}}46^{\mathrm{m}}43\overset{\mathrm{s}}{.}62$, $\delta = +41^\circ20'28\overset{''}{.}2$, J2000) is a single-line spectroscopic binary with the period of $P_{\mathrm{SB}} = 1\overset{\mathrm{d}}{.}2868$ days and eccentric orbit with $e = 0.1523$. We analyzed its TESS light curve with FAMIAS and found that the star showed small-amplitude ($0\overset{\mathrm{m}}{.}002$–$0\overset{\mathrm{m}}{.}003$) variability with the period of $P = 12\overset{\mathrm{d}}{.}18 \pm 0\overset{\mathrm{d}}{.}06$ days. The normalized light curve and the simple sinusoidal model are plotted in Fig. 7. Thus, we find that the photometric period differs from the period $P_{\mathrm{SB}}$ of the spectroscopic binary.

Taking into account three quantities, namely the period, amplitude, and spectral type, the star $d$ can be a BY Dra type variable of Class III (Chahal et al. 2022), and our measured period corresponds to the rotation period of one of its components. At the same time, the measurements of the H$\alpha$ line equivalent width (Zhang et al. 2020) did not show magnetic activity or variability in this system, so more information is needed

Table 2: Times of the primary minimum $T_{\rm min}$ = BJD − 2457000 and O–C values for the star *b1*

| $E$ | $T_{\rm min}$ Gauss fitting | $T_{\rm min}$ Minima27 | O–C |
|---|---|---|---|
| 0 | 2883.875 (0.003) | 2883.877 (0.002) | 0.0000 (0.0042) |
| 1 | 2885.670 (0.003) | 2885.672 (0.005) | 0.0007 (0.0059) |
| 2 | 2887.468 (0.003) | 2887.469 (0.002) | 0.0030 (0.0033) |
| 3 | 2889.256 (0.004) | 2889.258 (0.002) | -0.0033 (0.0039) |
| 4 | 2891.051 (0.003) | 2891.053 (0.001) | -0.0030 (0.0032) |
| 5 | 2892.843 (0.004) | 2892.846 (0.006) | -0.0054 (0.0070) |
| 8 | 2898.230 (0.003) | 2898.229 (0.003) | -0.0046 (0.0040) |
| 9 | 2900.027 (0.002) | 2900.026 (0.003) | -0.0028 (0.0039) |
| 10 | 2901.820 (0.002) | 2901.820 (0.002) | -0.0037 (0.0029) |
| 12 | 2905.415 (0.002) | 2905.417 (0.006) | 0.0028 (0.0068) |
| 13 | 2907.209 (0.002) | 2907.209 (0.001) | 0.0004 (0.0028) |
| 14 | 2909.000 (0.003) | 2908.999 (0.002) | -0.0037 (0.0036) |

for the star *d*.

#### 3.1.5 The star *e*: 2MASS J02465622+4117392 or 2MASS J02465472+4118213?

In Maíz Apellániz et al. (2023), the star 2MASS J02465622+4117392 (the star *e*) ($\alpha = 02^{\rm h}46^{\rm m}56^{\rm s}.22, \delta = +41°17'39''.3$, J2000) has the VARF parameter as "non-variable" or "marginal". The TESS light curve shows very similar variability (but with different trends in four time intervals) for two stars: the star *e* and 2MASS J02465472+4118213 (the star *e1*). The angular distance between these stars is 47″.8. The radii of the best photometric apertures for the stars *e* and *e1* are 52″.6 and 63″, so both apertures contain both stars. After aligning, the light curve of the star *e* shows that its variability is slightly larger than for the star *e1*. That is why we guess that our variable is the star *e*. The analysis with FAMIAS gave us 4 frequencies and the main one, with the largest amplitude, is $f_1 = 0.2505 \pm 0.0006$ c d$^{-1}$, the corresponding period being $P = 4^{\rm d}.022 \pm 0^{\rm d}.009$ days. The other frequencies are $f_2 = 0.348 \pm 0.002$ c d$^{-1}$, $f_3 = 0.2020 \pm 0.0009$ c d$^{-1}$, and $f_4 = 0.308 \pm 0.002$ c d$^{-1}$. Figure 8 shows the TESS light curve with the synthetic model using 4 frequencies and the phased light curve. Taking into account the star's period, amplitude, and spectral classification. we conclude that this star is probably an ellipsoidal binary.

### 3.2 The field of CV Boo

#### 3.2.1 The star *f*: 2MASS J15273711+3703070

After cross-identification of the stars in the CV Boo field with ATLAS and ZTF catalogs of suspected variable stars, the star *f* ($\alpha = 15^{\rm h}27^{\rm m}37^{\rm s}.11,\ \delta = +37°03'07''.1$, J2000) that is contained in both catalogs has been analyzed. The analysis of the MAO light curves confirmed the star's variability. Typical uncertainties of the instrumental magnitudes for the new variable star, $\sim 0^{\rm m}.03 - 0^{\rm m}.04$, are large enough because of its low brightness relative to the reference star, with formal photometric error $\sim 0^{\rm m}.004$, which is why we do not show the uncertainties in the left panel of Fig. 9. The ZTF catalog gives the

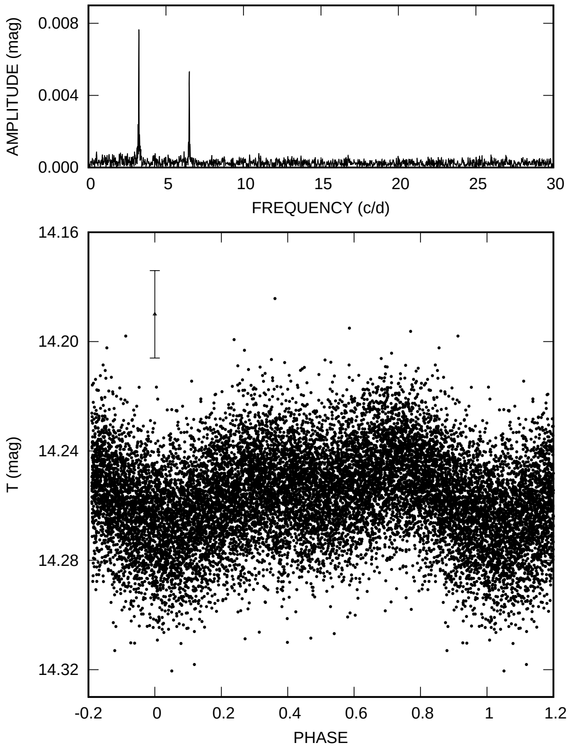


**Figure 6.**
Top panel: Fourier spectrum for the star $c$ that shows only two frequencies. Bottom panel: TESS light curve of the star 2MASS J02475840+4116103 (the star $c$) folded with the period of $0\overset{d}{.}30744$.

possible periods of $925\overset{d}{.}45242$ and $933\overset{d}{.}15749$, the ATLAS catalog gives the periods of $P_{\rm LF} = 627\overset{d}{.}616333$, $P_{\rm SF} = 0\overset{d}{.}99216$, and $P_{\rm LS} = 0\overset{d}{.}330726$, with "dubious" classification.

Unfortunately, the light curves available in ATLAS, ZTF, and SWASP surveys have data that are insufficient for proper analysis. That is why, despite the noisy light curve, the frequency analysis of the star $f$ with FAMIAS was done using the MAO dataset. Three frequencies exceed the level of significance of $4\sigma$, namely 6.0467 c $d^{-1}$, 3.0019 c $d^{-1}$, and 3.01925 c $d^{-1}$. The ratios are $f_1/f_2 = 2.01$ and $f_1/f_3 = 2.00$, which indicates a binary star. The corresponding period is $P = 0\overset{d}{.}3307 \pm 0\overset{d}{.}0002$. In Fig. 9 (left panel), we plotted the normalized and smoothed MAO phased light curves of the variable and comparison stars folded with this period. Taking into account the spectral type, period, and low amplitude, we conclude that this is an ellipsoidal binary star exhibiting the O'Connell effect (O'Connell 1951). The ATLAS light curve folded with the same period and initial epoch as for MAO data is shown in the right panel of Fig. 9. The ZTF light curve is noisier but shows a distinct difference in the depth of the secondary minimum. An assumption about the binary nature of this star is supported by its inclusion in the list of new binary and variable star candidates detected by LAMOST (Qian et al. 2019) because of radial velocity difference of $\Delta$RV = 28.6 km s$^{-1}$. At the same time, the object was classified as an RS CVn star in GAIA DR3 (Maíz Apellániz et al. 2023) catalog, but without supporting information like the period.

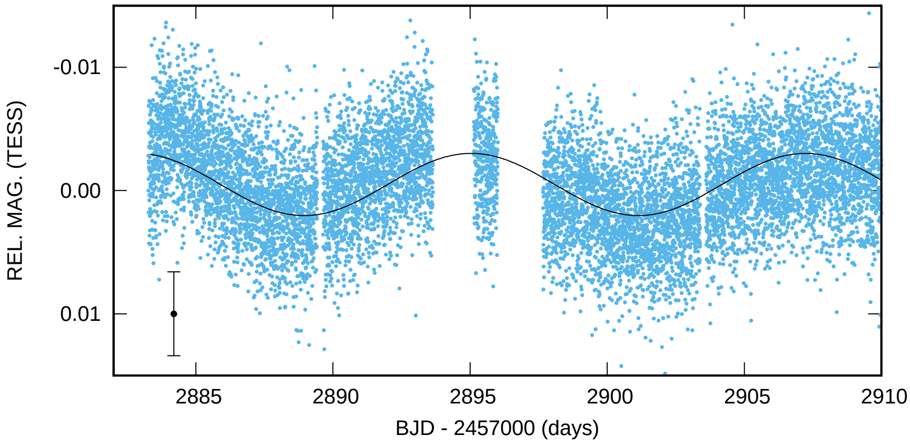


**Figure 7.**
TESS light curve of the star 2MASS J02464361+4120282 (the star *d*) and the synthetic curve.

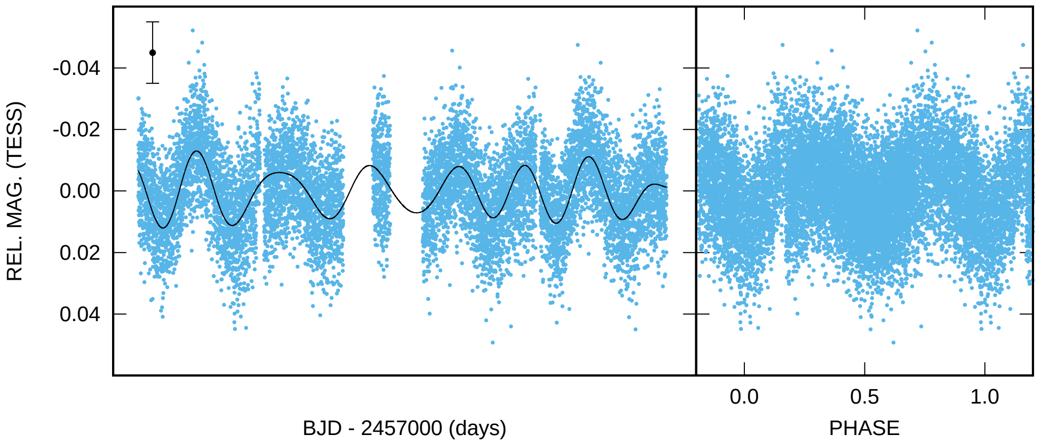


**Figure 8.**
TESS light curve of the star 2MASS J02465622+4117392 (the star *e*) with the synthetic model (left panel) and the phase light curve folded with the period 4.022 days (right panel).

## 4 Discussion and Conclusions

The archives of monitoring observations of two eclipsing binary stars obtained at Mt. Maidanak observatory were studied to search for new variable stars and in order to determine their variability types. The stars in the fields were cross-matched with the catalogs of suspected variable stars; publicly available light curves from the TESS mission and other surveys were studied. In Table 3, we present some observational and physical characteristics of the studied stars from the literature. The information in columns 2–4 is taken from GAIA DR3 or TESS Input Catalog (Stassun et al. 2019), the photometric magnitudes and colors in columns 6 and 7 are from the AAVSO Photometric All Sky Survey or ASCC-2.5 (Kharchenko 2001).

In Fig. 10, we show the locations of studied stars in the color–magnitude diagram. All six stars are main-sequence dwarfs, four of them have spectral types G2–G8, and two others have K3 and M3–M4 types. Such locations, combined with other characteristics, show that the nature of the brightness variability is not pulsations. The final result of our analysis is as follows.

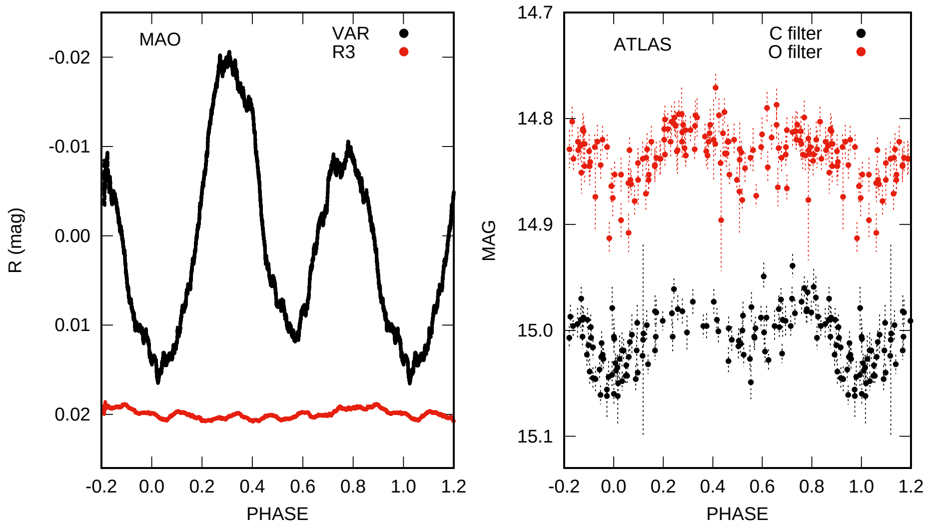


**Figure 9.**
Left panel: the smoothed normalized phase MAO light curves of the variable star *f* and comparison star. The light curve of the star R3 was shifted by $+0\overset{\mathrm{m}}{.}02$. Right panel: the ATLAS light curves of the star *f*. The curve in filter $O$ was shifted by $+0\overset{\mathrm{m}}{.}15$. The same period $P = 0\overset{\mathrm{d}}{.}3307$ and initial epoch $\mathrm{HJD}_0$=2456803.2425 were used.

Table 3: Parameters of the studied stars

| Star | $T_{eff}$ (K) | $R$ ($R_\odot$) | $M$ ($M_\odot$) | $D$ (pc) | $V$ (mag) | $B-V$ (mag) |
|---|---|---|---|---|---|---|
| a | 5435.5 | 1.39 | 0.94 | 966 | | |
| b | 4669.9 | 0.96 | | 642 | 15.28 | 0.92 |
| c | 3329.8 | 0.35 | 0.34 | 99 | | |
| d | 5728.1 | 1.02 | 1.04 | 345 | 12.63 | 0.70 |
| e | 5696.4 | 1.56 | 0.98 | 808 | 13.87 | 0.74 |
| f | 5656.1 | 1.48 | 1.01 | 1298 | 14.95 | 0.66 |

2MASS J02465266+4125290 is a detached eclipsing binary star with the period of $P = 5\overset{\mathrm{d}}{.}9436 \pm 0\overset{\mathrm{d}}{.}0027$. The depths of minimum I and minimum II are at least $0\overset{\mathrm{m}}{.}59$ and $0\overset{\mathrm{m}}{.}16$ in Bessel $R$ filter.

2MASS 02461044+4123154 is a detached eclipsing binary star with $P = 1\overset{\mathrm{d}}{.}794 \pm 0\overset{\mathrm{d}}{.}008$. The depth of the primary minimum is about $0\overset{\mathrm{m}}{.}4$ (ZTF $r$ filter).

2MASS J02475840+4116103 is an ellipsoidal binary star. $P = 0\overset{\mathrm{d}}{.}30744 \pm 0\overset{\mathrm{d}}{.}00005$, depths of minima are less than $0\overset{\mathrm{m}}{.}02$.

2MASS J02464361+4120282 is a spectroscopic binary containing a variable star of the BY Dra type with the rotation period of $P = 12\overset{\mathrm{d}}{.}18 \pm 0\overset{\mathrm{d}}{.}06$. The variability amplitude is less than $0\overset{\mathrm{m}}{.}01$.

2MASS J02465622+4117392 is an ellipsoidal binary star. $P = 4\overset{\mathrm{d}}{.}022 \pm 0\overset{\mathrm{d}}{.}009$, the amplitude is less than $0\overset{\mathrm{m}}{.}02$.

2MASS J15273711+3703070 is an ellipsoidal and/or RS CVn binary system (perhaps an ellipsoidal binary system with one or two active components). $P = 0\overset{\mathrm{d}}{.}3307 \pm 0\overset{\mathrm{d}}{.}0002$, the amplitude is at least $0\overset{\mathrm{m}}{.}04$.

**Acknowledgements.** This research has made use of the SIMBAD database, operated

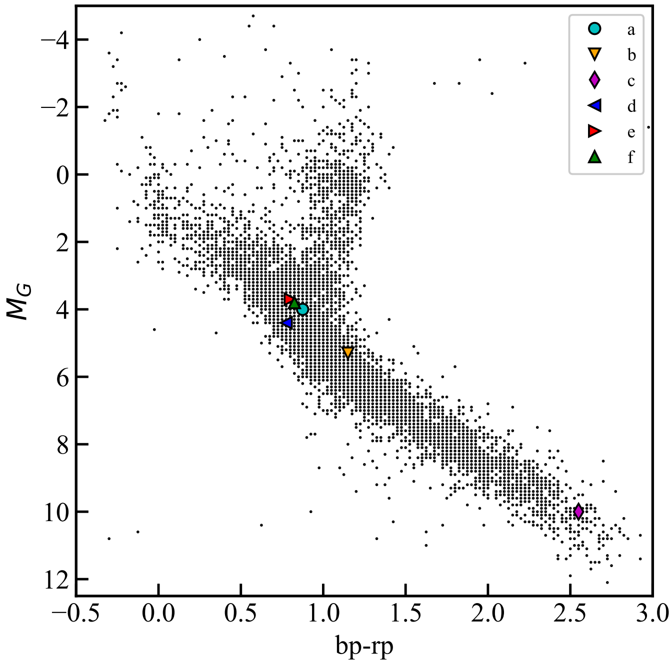


**Figure 10.**
Extinction-corrected color–magnitude diagram, with the stars studied in this work marked. The grey points are 100000 randomly selected stars from GAIA DR3 (with high-quality parallaxes: *parallax_over_error*>5).

at CDS, Strasbourg, France. This research has made use of the VizieR catalog access tool, CDS, Strasbourg, France. The original description of the VizieR service was published in Ochsenbein et al. (2000). This work has made use of data from the European Space Agency (ESA) mission Gaia[4], processed by the Gaia Data Processing and Analysis Consortium (DPAC[5]). Funding for the DPAC has been provided by national institutions, in particular, the institutions participating in the Gaia Multilateral Agreement. This paper includes data collected with the TESS mission, obtained from the Mikulski Archive for Space Telescopes (MAST) at the Space Telescope Science Institute (STScI). Funding for the TESS mission is provided by the NASA Explorer Program. STScI is operated by the Association of Universities for Research in Astronomy, Inc., under NASA contract NAS 526555. Support for MAST for non-HST data is provided by the NASA Office of Space Science via grant NNX13AC07G and by other grants and contracts. We thank the observers O. Parmonov, O. Abdullaev, and T. Boyqobilov.

References:

Bogomazov, A. I., Ibrahimov, M. A., Satovskii, B. L., et al. 2016a, *Astrophysics & Space Science*, **361**, article id. 4

Bogomazov, A. I., Kozyreva, V. S., Satovskii, B. L., et al. 2016b, *Astrophysics & Space Science*, **361**, article id. 390

Butters, O. W., West, R. G., Anderson, D. R., et al. 2010, *Astron. & Astrophys.*, **520**, article id. L10

[4]https://www.cosmos.esa.int/gaia
[5]https://www.cosmos.esa.int/web/gaia/dpac/consortium

Cantat-Gaudin, T., Vallenari, A., Sordo, R., et al. 2018, *Astron. & Astrophys.*, **615**, article id. A49

Chahal, D., de Grijs, R., Kamath, D., & Chen, X. 2022, *Monthly Notices Roy. Astron. Soc.*, **514**, No. 4, 4932

Chen, X., Wang, S., Deng, L., et al. 2020 *Astrophys. J., Suppl. Ser.*, **249**, article id. 18

Duerbeck, H. W. 1975, *Acta Astronomica*, **25**, No. 4, 361

Gaia Collaboration, Brown, A. G. A., Vallenari, A., Prusti, T., et al. 2021 *Astron. & Astrophys.*, **649**, article id. A1

Gaynullina, E. R., Khalikova, A. V., Serebryanskiy, A. V., et al. 2019, *Open European Journal on Variable Stars*, **202**, 1

Heinze, A. N., Tonry, J. L., Denneau, L., et al. 2018, *Astron. J.*, **156**, article id. 241

Henden, A. A., Levine, S., Terrell, D., & Welch, D. L. 2015, *American Astronomical Society, AAS Meeting*, **225**, id. 336.16

Khalikova, A., Gaynullina, E., & Serebryanskiy, A. 2022, *New Astronomy*, **97**, article id. 101875

Kharchenko, N. V. 2001 *Kinematika i Fizika Nebesnykh Tel*, **17**, No. 5, 409

Maíz Apellániz, J., Holgado, G., Pantaleoni González, M., & Caballero, J. A. 2023, *Astron. & Astrophys.*, **677**, article id. A137

O'Connell, D. J. K. 1951, *Monthly Notices Roy. Astron. Soc.*, **111**, No. 6, 642

Ochsenbein, F., Bauer, P., & Marcout, J. 2000, Âstron. & Astrophys., Suppl. Ser., **143**, No. 1, 32

Parimucha, Š., Gajdoš, P., Kudak, V., et al. 2018, *Research in Astron. & Astrophys.*, **18**, No. 4, article id. 047

Pelt, J., Hoff, W., Kayser, R., et al. 1994, *Astron. & Astroph.*, **286**, No. 3, 775

Pelt, J., Kayser, R., Schild, R., & Thomson, D. J. 1996, *Proceedings of the IAU Symposium 168*, eds. M. C. Kafatos & Y. Kondo, p. 539

Pourbaix, D., Arenou, F., Gavras, P., et al. 2022, *Gaia DR3 documentation, European Space Agency; Gaia Data Processing and Analysis Consortium. Online at https://gea.esac.esa.int/archive/documentation/GDR3/index.html*, id. 7

Qian, S.-B., Shi, X.-D., Zhu, L.-Y., et al. 2019, *Research in Astron. & Astrophys.*, **19**, No. 5, article id. 064

Southworth, J., Maxted, P. F. L., & Smalley, B. 2004, *Monthly Notices Roy. Astron. Soc.*, **351**, No. 4, 1277

Stassun, K.G., Oelkers, R. J., Paegert, M., et al. 2019, *Astron. J.*, **158**, article id. 138

Tutukov, A. V. & Bogomazov, A. I. 2012, *Astronomy Reports*, **56**, No. 10, 775

Zhang, L.-Y., Long, L., Shi, J., et al. 2020, *Monthly Notices Roy. Astron. Soc.*, **495**, No. 1, 1252

Zima, W. 2008, *Communications in Asteroseismology*, **157**, 387